Learning Catheter-Aorta Interaction Model Using Joint Probability Densities

Yohannes Kassahun, Bingbin Yu
University of Bremen
Faculty 3 - Mathematics and Computer Science
Mary-Somerville-Str. 9, D-28359 Bremen, Germany
Email: kassahun@informatik.uni-bremen.de

Emmanuel Vander Poorten
University of Leuven
Dept. of mechanical engineering, division PMA
Celestijnenlaan 300B, B-3001 Heverlee, Belgium

I. Abstract

Catheter based diagnosis and therapy of cardiovascular diseases is becoming more popular these days. Often the vasculature is being accessed from a less invasive location remote to the cardiac region. For transfemoral approaches of TAVI procedures the vasculature is for example accessed through a cannula inserted into the patient's groin and then moved gently up to the heart [1]. Due to the complex and deformable nature of both the vasculature and the catheter, the overall controllability of the catheter itself is low in such a case. Tissue damage, dissection or perforation of the vessel and even of the heart cannot be ruled out [2], [3], [4]. The Cognitive AutonomouS CAtheter operating in Dynamic Environments (CASCADE) [5], a recent EU-funded FP7 project, investigates autonomous catheter control and explores machine learning techniques to learn the input-output behavior of the catheter inside vessels of artificial mock-ups. The results from this study should enhance the understanding, the control of catheter motion and interaction patterns also during real interventions.

Before learning to control a catheter, different ways of learning the interaction model of the catheter with the aorta should be investigated. These will help to transfer the learned model from the mock-up to the real world in the long run. Since it is not always possible to guarantee safety when applying learning methods, it is important to first investigate different ways of learning the catheter-aorta interaction model and evaluate their failure modes.

II. Experimental Setup

A two dimensional mock-up of the aorta was constructed; the mock-up together with an RFA ablation catheter (EndoSense SA) is shown in Figure 1. An exact replica of this exact mock-up is distributed among the partners of the CASCADE project so that algorithms can be shared freely. In addition to this, partners can compare their results or even reproduce results of other partners. The mock-up of the aorta is a rigid body, which is a very simple model of the aorta. Since the mock-up is a rigid body, the properties of the catheter-aorta interaction will mainly depend on the catheter. As a sensor a camera was used. The camera looks straight down to the plane in which the aorta is lying. It is a high-resolution network camera (AXIS 215 PTZ). The PTZ network camera provides pan, tilt and zoom functions, enabling wide area coverage and easy manipulation through web browsers. The camera is mounted directly above the testbed at a height of 56 centimeters. The resolution of the video image is 704×576 pixels for the 4CIF format. The upper and lower boundaries of the aorta in the testbed are colored in pink and yellow, respectively. This marking simplifies the identification by image processing. Figure 2 shows the catheter and the mock-up as seen from the camera perspective. From the camera image, the following parameters are extracted: (1) the shape of the catheter, (2) the contact points where the catheter touches the boundaries of the aorta in different

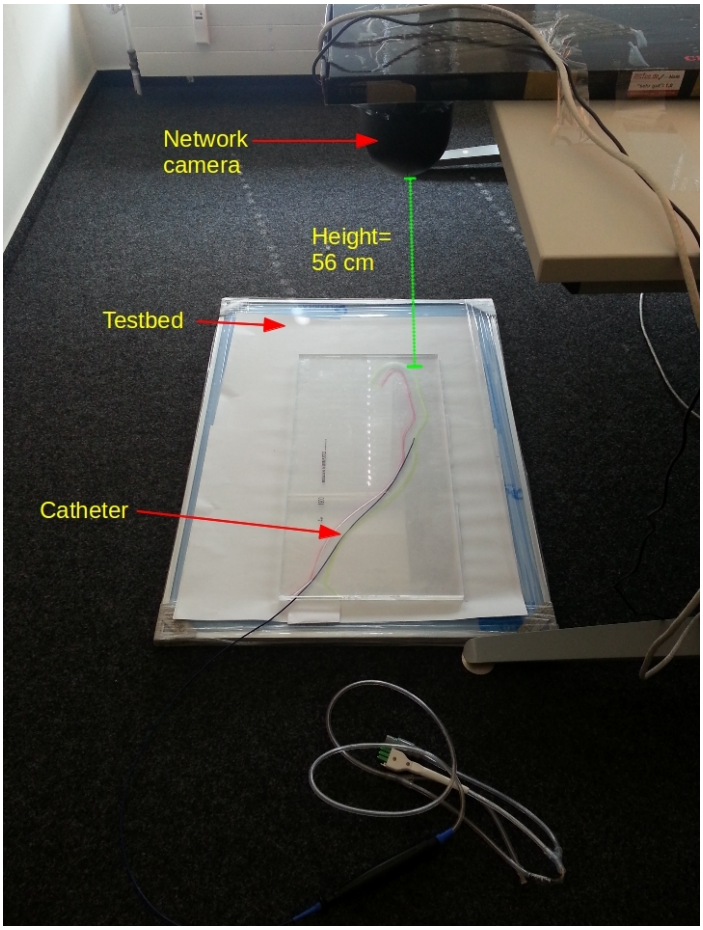

Fig. 1. The experimental setup. In the picture the mock-up, a commercial catheter and a camera used to measure the catheter are shown.

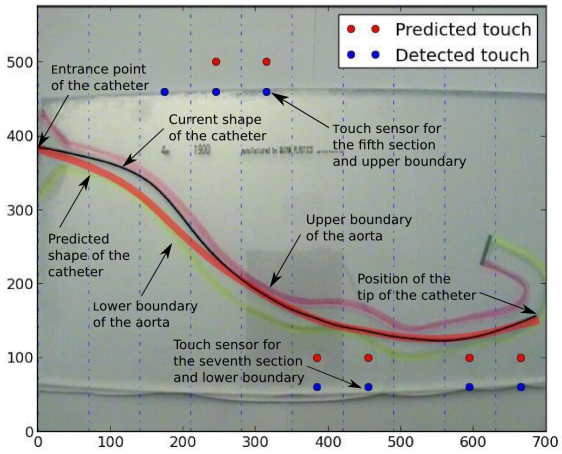

Fig. 2. The mock-up and the catheter as seen from the camera perspective. The different parameters that are used for modeling the catheter-aorta interaction are shown. The numbers on the horizontal and vertical axes show the pixel coordinates in the image. The dotted vertical lines in the image show the boundaries of the different sections. The red dots above and below the aorta show the state of the touch sensors.

sections, (3) the entrance point of the catheter and (4) the tip of the catheter. For the purpose of extracting the parameters listed above, we used an OpenCV implementation programmed in the Python programming language[6].

III. Method

In this paper we present a catheter-aorta interaction modeling using joint probability densities [7]. For modeling training data is collected using the above-mentioned camera setup. The training data is gathered by applying different manipulation acts on the catheter (mainly pushing the catheter into and pulling the catheter out of the mock-up). Each entry in the training data has five components. The first component is a vector of contact points of different sections of the catheter for the upper boundary of the aorta $\boldsymbol{t}_u$. The second component is a vector of contact points of different sections of the catheter for the lower boundary of the aorta $\boldsymbol{t}_l$. The dimension of the vectors for the touch sensors of the upper and lower boundaries of the aorta is equal to the number of sections. For this experiment the aorta was subdivided into ten sections. Figure 2 shows dotted vertical lines representing the boundaries of the different sections. The third component is a vector of coefficients of a function $\boldsymbol{\alpha}$ used to represent the shape of the catheter. In this work, we used B-splines of third order to approximate the shape of the catheter. The number of coefficients for approximating the shape of the catheter is 34, which corresponds to 30 splines. The fourth and fifth components represent the Cartesian coordinates (expressed in pixels) of the entrance point of the catheter $\boldsymbol{p}_e$ and the tip of the catheter $\boldsymbol{p}_t$, respectively. During training the joint probability distribution

$$p(\boldsymbol{t}_u, \boldsymbol{t}_l, \boldsymbol{\alpha}, \boldsymbol{p}_e, \boldsymbol{p}_t), \tag{1}$$

is learned and during testing from the joint probability distribution

$$\mathbb{E}\left[\boldsymbol{\alpha} | \boldsymbol{p}_e, \boldsymbol{p}_t\right], \tag{2}$$

is calculated, where $\mathbb{E}$ stands for expected value. Expression (2) gives the estimate of the current shape of the catheter given $\boldsymbol{p}_e$ and $\boldsymbol{p}_t$ by generating the shape of the catheter from the coefficients $\boldsymbol{\alpha}$. In reality $\boldsymbol{p}_e$ is more or less known and $\boldsymbol{p}_t$ could be e.g. acquired from an electromagnetic sensor embedded in the catheter tip. Here, this sensor is simulated through our camera measurements. Note that the model (1) implicitly incorporates the geometry of the vessel. For different vessel geometries this model thus needs to be updated. Now, the state of the touch sensors can then be estimated using

$$\mathbb{E}\left[\boldsymbol{t}_u, \boldsymbol{t}_l | \boldsymbol{p}_e, \boldsymbol{p}_t\right], \tag{3}$$

which can also be calculated from expression (1). If the shape of the catheter is known, then the state of the touch sensors can be estimated using

$$\mathbb{E}\left[\boldsymbol{t}_u, \boldsymbol{t}_l | \boldsymbol{\alpha}, \boldsymbol{p}_e, \boldsymbol{p}_t\right]. \tag{4}$$

To calculate analytically the quantities given by expressions (2), (3) and (4), we used a mixture of Gaussians for modeling the joint probability distribution given by expression (1). Mixture of Gaussians are discussed at length in the book by Mclachlan and Peel [8].

IV. Results

After training the catheter-aorta interaction model, the model is evaluated for its prediction capabilities for the shape of the catheter and the states of touch sensors for all sections of the aorta and for the upper and lower boundaries of the aorta. The evaluation is performed on a novel dataset, which is not included in the training set. Figure 3 shows the prediction performance of the model in predicting the shape of the catheter using expression (2) and the state of the touch sensors for the upper and lower boundaries of the aorta for some of the positions of the tip of the catheter using expression (3). As can be seen from these results, the model is able to predict

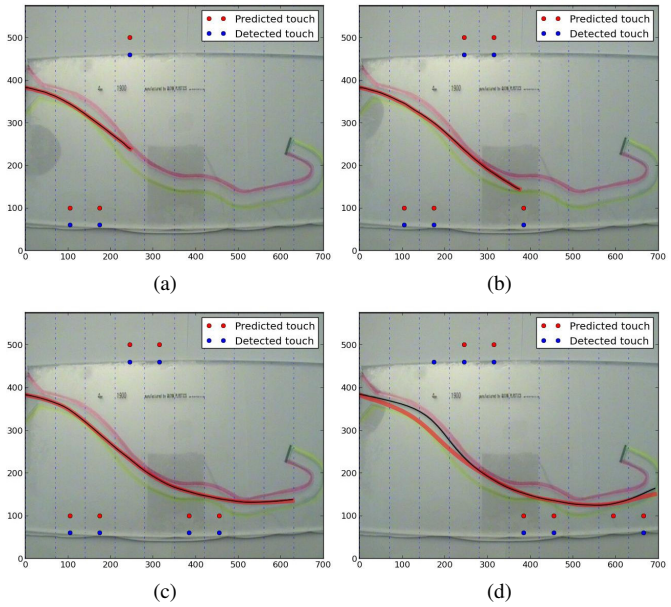

Fig. 3. The predictions of the shape of the catheter and the state of the touch sensors for the upper and lower boundaries of the aorta.

the shape of the catheter and the state of the touch sensors in the different sections of the catheter.

In the following we examine the prediction given by expression (4) more closely since in reality the shape of the catheter can be extracted from electromagnetic sensors embedded along the catheter, or from fluoroscopic images. During testing, for each section i we counted the number of times a touch sensor corresponding to section i and the upper boundary detects touch, $\#T_{ui}$, and the number of times a touch sensor corresponding to section i and the lower boundary detects touch, $\#T_{li}$. We calculated the true positive rates TPR_{ui} and TPR_{li} for the upper and lower boundaries and for section i using

$$TPR_{ui} = \frac{\#\left((\text{prediction}_{ui}\text{= touch}) \wedge (\text{sensor}_{ui}\text{ = touch})\right)}{\#T_{ui}}, \tag{5}$$

$$TPR_{li} = \frac{\#\left((\text{prediction}_{li}\text{= touch}) \wedge (\text{sensor}_{li}\text{ = touch})\right)}{\#T_{li}}. \tag{6}$$

Similarly, we counted the number of times a touch sensor corresponding to section i and the upper boundary detects no touch, $\#NT_{ui}$, and the number of times a touch sensor corresponding to section i and the lower boundary detects no touch, $\#NT_{li}$. We then calculated true negative rates TNR_{ui} and TNR_{li} for the upper and lower boundaries and for section i using

$$TNR_{ui} = \frac{\#((\text{prediction}_{ui}\text{=no touch}) \wedge (\text{sensor}_{ui}\text{ =no touch}))}{\#NT_{ui}}, \tag{7}$$

$$TNR_{li} = \frac{\#((\text{prediction}_{li}\text{=no touch}) \wedge (\text{sensor}_{li}\text{ =no touch}))}{\#NT_{li}}. \tag{8}$$

Then we calculated the harmonic mean accuracy (HMACC) for section i and the upper and lower boundaries using

$$\text{HMACC}_{ui} = \frac{2(TPR_{ui}\, TNR_{ui})}{TPR_{ui} + TNR_{ui}}, \tag{9}$$

$$\text{HMACC}_{li} = \frac{2(TPR_{li}\, TNR_{li})}{TPR_{li} + TNR_{li}}. \tag{10}$$

The values for the HMACC lie between zero and one. A higher value of HMACC means a better prediction accuracy. Standard accuracy measures for section i and the upper and lower boundaries given by

$$\text{Accuracy}_{ui} = \frac{TPR_{ui}\#T_{ui} + TNR_{ui}\#NT_{ui}}{\#T_{ui} + \#NT_{ui}}, \tag{11}$$

$$\text{Accuracy}_{li} = \frac{TPR_{li}\#T_{li} + TNR_{li}\#NT_{li}}{\#T_{li} + \#NT_{li}} \tag{12}$$

are also calculated. If the number of touches detected by the touch sensor for section i and a boundary is different from the number of no touches, then the HMACC gives high values for models predicting well both the touch and non touches. If a model predicts correctly all the non touches but predicts incorrectly all of the touches, it gets an HMACC value of 0. However, the same model might get a high value of accuracy. This is evident from the HMACC and accuracy values for section $S6$ of the upper boundary shown in Figure 4. As can be seen from the figure, the model detects the states of the touch sensors most of the times correctly. In the future, the deformable and variable nature of the vessel will need to be addressed.

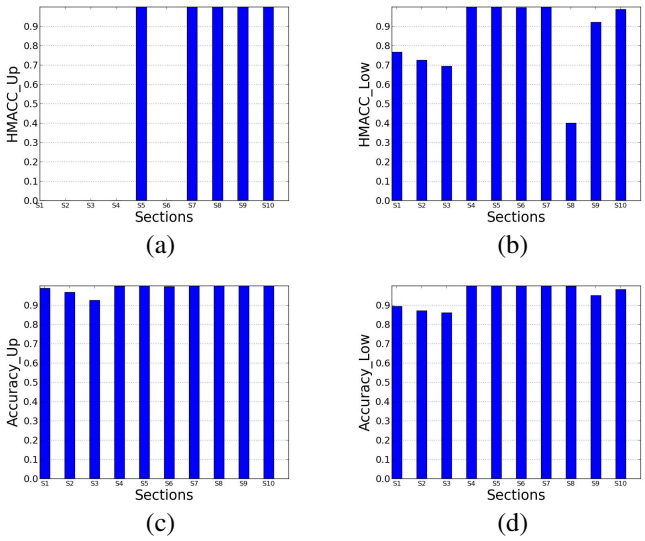

Fig. 4. The harmonic mean values and accuracies for each section and for the upper (a) & (c) and lower (b) & (c) boundaries of the aorta, respectively.

REFERENCES

[1] W. Gaasch and R. D'Agostino, "Transcatheter aortic valve implantation: The transfemoral versus the transapical approach." *Ann Cardiothorac Surg*, pp. 200–205, 2012.

[2] T. Kono, H. Kitahara, M. Sakaguchi, and J. Amano, "Cardiac rupture after catheter ablation procedure." *The Annals of Thoracic Surgery*, vol. 80, no. 1, pp. 326–327, 2005. [Online]. Available: http://www.ncbi.nlm.nih.gov/pubmed/15975397

[3] R. Tilz, K. Chun, A. Metzner, A. Burchard, E. Wissner, B. Koektuerk, M. Konstantinidou, D. Nuyens, T. De Potter, K. Neven, A. Furnkranz, F. Ouyang, and B. Schmidt, "Unexpected high incidence of esophageal injury following pulmonary vein isolation using robotic navigation," *Journal of Cardiovascular Electrophysiology*, vol. 21, no. 8, pp. 853–858, August 2010.

[4] A. Aminian, J. Lalmand, and B. El Nakadi, "Perforation of the descending thoracic aorta during transcatheter aortic valve implantation (tavi): An unexpected and dramatic procedural complication," *Catheterization and Cardiovascular Interventions*, vol. 77, no. 7, pp. 1076–1078, 2011.

[5] "Cognitive AutonomouS CAtheter operating in Dynamic Environments (CASCADE)," http://www.cascade-fp7.eu/, [Online; accessed August 30 2013].

[6] G. Bradski, "The OpenCV Library," *Dr. Dobb's Journal of Software Tools*, 2000.

[7] M. Edgington, Y. Kassahun, and F. Kirchner, "Using joint probability densities for simultaneous learning of forward and inverse models," in *IEEE IROS International Workshop on Evolutionary and Reinforcement Learning for Autonomous Robot Systems*, N. T. Siebel and J. Pauli, Eds., 10 2009, pp. 19–22.

[8] G. Mclachlan and D. Peel, *Finite Mixture Models*, 1st ed., ser. Wiley Series in Probability and Statistics. Wiley-Interscience, 2000.